High degree of molecular orientation by a combination of THz and femtosecond laser pulses

Kenta Kitano, Nobuhisa Ishii, and Jiro Itatani

Institute for Solid State Physics, University of Tokyo, 5-1-5 Kashiwanoha, Kashiwa, Chiba 277-8581, Japan and CREST, Japan Science and Technology Agency, 5 Sanbancho, Chiyoda-ku, Tokyo 102-0075, Japan

(Received 2 July 2011; published 11 November 2011)

We propose a method for achieving molecular orientation by two-step excitation with intense femtosecond laser and terahertz (THz) pulses. First, the femtosecond laser pulse induces off-resonant impulsive Raman excitation to create rotational wave packets. Next, a delayed intense THz pulse effectively induces resonant dipole transition between neighboring rotational states. By controlling the intensities of both the pulses and the time delay, we can create rotational wave packets consisting of states with different parities in order to achieve a high degree of molecular orientation under a field-free condition. We numerically demonstrate that the highest degree of orientation of $\langle \cos\theta \rangle > 0.8$ in HBr molecules is feasible under experimentally available conditions.

DOI: 10.1103/PhysRevA.84.053408 PACS number(s): 33.80.−b, 42.50.Hz

I. INTRODUCTION

Manipulation of the rotational freedom in gas-phase molecules has long been an important subject in the study of reaction dynamics. It is roughly classified into two types: alignment and orientation. Alignment refers to the rotational states in which the symmetry axis of a molecule is localized along a laboratory-fixed axis, whereas orientation refers to the states in which the upward and downward directions of the axis are additionally controlled. Techniques for molecular alignment have been well developed by applying nonresonant laser pulses with nanosecond to femtosecond durations [1]. When the pulse duration τ is sufficiently longer than molecular rotational periods $\tau_{\rm rot}$, i.e., $\tau \gg \tau_{\rm rot} = h/2B_{\rm e}$, where $B_{\rm e}$ is the rotational constant, the molecules are adiabatically aligned in the presence of laser fields. This alignment is retained only during the laser pulse [2]. On the other hand, when the pulse duration is shorter than the rotational periods, i.e., $\tau \ll \tau_{\rm rot}$, rotational wave packets are created through impulsive Raman processes. In this case, molecules are periodically aligned under field-free conditions even after the propagation of the excitation pulse [3,4]. The nonadiabatic methods have been extensively applied in various strong-field experiments, such as alignment dependencies of field ionizations [5], high harmonic generation [6,7], and angular momentum orientation [8]. These methods have also become the basis of molecular-orbital tomography [9] and laser-induced electron diffraction [10].

Compared to the tremendous progress in alignment mentioned above, molecular orientation still remains a significant challenge. Until now, the methods that have been proposed and demonstrated include the use of a strong dc field ("brute-force orientation") [11], preparing state-selected molecules with hexapole focusing [12], dc and intense nonresonant laser fields [13–15], and phase-locked two-color laser fields [16,17]. The highest degree of orientation was achieved by a combination of the hexapole focusing with the dc and intense nonresonant laser fields [18]. The orientation degree, which is given by the ensemble average of $\cos\theta$, where θ is the angle between the laboratory-fixed and the molecular axes, reached up to $\langle \cos\theta \rangle \sim 0.74$. However, the number density of molecules was reduced through the state-selection process. Furthermore, the orientation was achieved in the presence of a dc field, which may perturb the quantum states of target molecules. The two-color laser fields can orient molecules under a field-free condition, but degrees of orientation are quite small.

In addition to these approaches, intense electric fields in the THz region have been considered to be a promising tool for realizing orientation with a reasonable number density of molecules under a field-free condition. There have been many proposals for molecular orientation using a half-cycle pulse (HCP) [19–23]. However, none of these proposals has been experimentally demonstrated because of the technical difficulty in generating intense HCPs. As a result of the recent breakthrough in THz technology, intense THz pulses have become easily obtainable via the pulse-front-matching technique in optical rectification [24] and the maximum field intensity of the THz pulses has recently reached the order of 1 MV/cm [25]. However, these intense THz pulses are nearly single-cycle pulses, and not half-cycle pulses, which are difficult to apply to the proposed methods using HCPs because the inversion asymmetry is not necessarily associated.

Based on these recent technological advances, we propose a method to achieve a high degree of molecular orientation using a single-cycle intense THz pulse in combination with a femtosecond laser pulse. In previous HCP methods, the sudden-impact approximation was often applied and the interaction with the electric field was treated as a directional momentum kick. While this model can provide an intuitive explanation of orientation dynamics, the most fundamental requisite for realizing orientation is to induce dipole transition between even- and odd-numbered rotational states [26]. In our method, the transition probability is enhanced by preexciting molecules with a nonresonant femtosecond laser pulse so that the transition frequency becomes resonant with the subsequent THz pulse. After the irradiations of both pulses, highly oriented states appear periodically as the wave packet evolves in the absence of external fields. By numerically solving a time-dependent Schrödinger equation in a rigid-rotor approximation, we obtained a high degree of molecular orientation of $\langle \cos\theta \rangle \sim 0.84$ in an HBr molecule that has a moderate permanent dipole moment.

This paper is organized as follows. Section II outlines the proposed method. Section III describes the simulated results and the orientation dynamics is discussed to clarify the mechanism of the orientation. Conclusions and perspectives are given in Sec. IV.

II. DESCRIPTION OF THE METHOD

A. Basic strategy of the method

The schematic of our method is shown in Fig. 1(a). First, a linearly polarized, intense, nonresonant femtosecond laser pulse creates rotational wave packets through impulsive Raman excitation according to the selection rule of $\Delta J = 0, \pm 2$, and $\Delta M = 0$, where J is the total angular momentum and M is its projection on a laboratory-fixed Z axis (defined parallel to the laser electric field). At this stage, the molecules are aligned but not oriented because of the lack of coherence between the even and odd J states, which have different parities. After a variable time delay, a nearly single-cycle THz pulse [Fig. 1(b)], whose polarization is set parallel to the femtosecond laser field, is applied to induce a resonant dipole transition between the even and odd states according to the selection rule of $\Delta J = \pm 1$ and $\Delta M = 0$. The maximum degree of molecular orientation is realized under a field-free condition during the evolution of the wave packets.

This scheme has two advantages over the other orientation schemes using HCPs or THz pulses. We explain them using an HBr molecule whose rotational constant is $B_e = 8.3482\ \mathrm{cm}^{-1}$ [27]. The energy spacings between neighboring rotational states up to $J = 4$ are located in the THz pulse spectrum, as shown in Fig. 1. First, the nonresonant femtosecond laser pulse excites molecules from $J = 0$ to $J = 2,4$ states. This preexcitation enables effective population transfer to the $J = 3$ state through dipole transition induced by the THz pulse. The contribution of higher rotational states with different parities, such as the $J = 3$ state, plays an important role in achieving a higher degree of orientation. Without this preexcitation, it is difficult to excite molecules from $J = 0$ to higher J ($\geqslant 2$) states with the THz pulse alone because these excitations become multiphoton processes under the selection rule of $\Delta J = \pm 1$. The second advantage is the controllability of quantum interference. The preexcitation with the nonresonant femtosecond pulse and the irradiation of the following THz pulse create several excitation pathways from $J = 0$ to $J = 1,3$ states, as indicated in Fig. 1(a). To achieve the highest degree of molecular orientation, we can optimize the quantum interference of these pathways by changing the intensity of the femtosecond and THz pulses as well as the time delay between them.

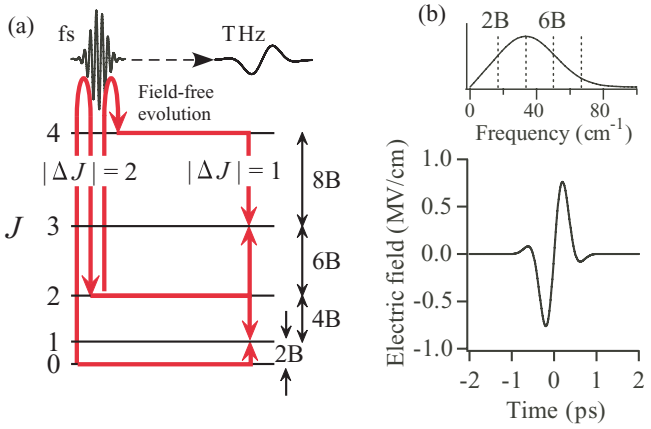

FIG. 1. (Color online) (a) Schematic representation of rotational transitions by nonresonant femtosecond laser and resonant THz pulses. (b) Temporal shape of the THz pulse. The upper part shows its spectrum and the energy spacings between neighboring rotational states of HBr.

B. Calculation details

We investigate the orientation dynamics of the HBr molecule irradiated by linearly polarized femtosecond laser and THz pulses with their polarization axes set parallel. The time evolution of a rotational wave function is given by solving a time-dependent Schrödinger equation,

$$i\hbar \frac{d\psi(t)}{dt} = \hat{H}(t)\psi(t). \tag{1}$$

We apply a rigid-rotor approximation in which vibrational motions are neglected and treat the radiation interaction in the dipole approximation. Then the Hamiltonians of the linear molecules irradiated by the THz and femtosecond laser pulses are given by Eqs. (2) and (3), respectively [19–23].

$$\hat{H}_{\mathrm{THz}}(t) = B_e \hat{J}^2 - \mu_0 \varepsilon_{\mathrm{THz}}(t)\cos\theta, \tag{2}$$

$$\begin{aligned}\hat{H}_{\mathrm{fs}}(t) &= B_e \hat{J}^2 - \frac{\varepsilon_{\mathrm{fs}}(t)^2}{2}(\Delta\alpha \cos^2\theta + \alpha_\perp) \\ &= B_e \hat{J}^2 - \frac{\varepsilon_{\mathrm{fs}}^{\mathrm{env}}(t)^2}{4}(\Delta\alpha \cos^2\theta + \alpha_\perp).\end{aligned} \tag{3}$$

$\hat{J}^2$ is the squared angular momentum operator, μ_0 is the permanent dipole moment, θ is the angle between the molecular axis and electric-field vectors $\varepsilon_{\mathrm{THz}}$ and $\varepsilon_{\mathrm{fs}}$, respectively, and $\varepsilon_{\mathrm{fs}}^{\mathrm{env}}$ is the envelope of $\varepsilon_{\mathrm{fs}}$. Polarizability anisotropy is defined as $\Delta\alpha = \alpha_{||} - \alpha_\perp$, where $\alpha_{||}$ and $\alpha_\perp$ are polarizability components parallel and perpendicular to the molecular axis, respectively. In Eq. (3), the rapid oscillations of the field are averaged out by applying a rotating wave approximation.

Next, we expand the rotational wave function using the finite basis set of $|J,M\rangle$, which is a set of the eigenfunctions of a rigid rotor in a field-free space. Because we defined the polarization axes of both the pulses as the laboratory-fixed Z axis, the Hamiltonian is cylindrically symmetric about the Z axis. Therefore, M becomes a good quantum number, that is, $\Delta M = 0$, and then the wave function is expressed as

$$|\psi(t)\rangle = \sum_{J=0}^{J_{\max}} c_{J,M}(t)|J,M\rangle \exp\left(-i\frac{E_J}{\hbar}t\right), \tag{4}$$

where $J_{\max}$ is set at the value which far exceeds the highest rotational states excited by both pulses and E_J is an eigenenergy of the $|J,M\rangle$ state, which depends only on J and not on M. By inserting the Hamiltonians in Eqs. (2) and (3) and the wave function in Eq. (4) into Eq. (1), it can be recast as an ensemble of coupled differential equations about the coefficient $c_{J,M}$. We solved these equations by applying the fourth-order Runge-Kutta method.

C. Estimation of orientation

The orientation dynamics can be estimated from the obtained wave function as follows:

$$\begin{aligned}\langle\cos\theta\rangle(t) &= \sum_{J=0}^{J_{\max}}\sum_{J'=0}^{J'_{\max}} |c_{J',M}c_{J,M}|\langle J',M|\cos\theta|J,M\rangle \\ &\quad\times\exp\left[i\left(\frac{\Delta E_{J',J}}{\hbar}t-\phi_{J',J}\right)\right] \\ &= 2\sum_{J=0}^{J_{\max}} |c_{J+1,M}c_{J,M}|\langle J+1,M|\cos\theta|J,M\rangle \\ &\quad\times\cos\left(\frac{\Delta E_{J+1,J}}{\hbar}t-\phi_{J+1,J}\right), \end{aligned} \tag{5}$$

where we used the evaluations of matrix elements $\langle J',M|\cos\theta|J,M\rangle = 0$ when $|J'-J|\neq 1$, which are derived from properties of spherical harmonics, and applied the following notations:

$$\begin{aligned}\Delta E_{J+1,J} &= E_{J+1}-E_J = 2B_e(J+1), \\ \phi_{J+1,J} &= \arg(c_{J+1,M})-\arg(c_{J,M}).\end{aligned} \tag{6}$$

From Eq. (5), it is obvious that the orientation dynamics includes several frequency components that correspond to energy differences between neighboring rotational states. The modulation amplitude of each component is determined by $|c_{J+1,M}c_{J,M}|$, and the offset phase $-\phi_{J+1,J}$ is determined by the relative phase between rotational states. The maximum degree of orientation can be achieved at the instant when the sinusoidal modulations of various angular frequencies, $\Delta E_{J+1,J}/\hbar$, are in phase with the nearly equal population of neighboring rotational states, i.e., $|c_J|\simeq|c_{J+1}|$. We will demonstrate how these conditions can be satisfied by controlling the intensity and time delay between the femtosecond laser and THz pulses.

It should be noted that molecules are oriented by interactions with the THz pulse, whose selection rule is $\Delta J=\pm 1$, and not by interactions with the femtosecond pulse, whose selection rule is $\Delta J = 0,\pm 2$.

III. SIMULATION RESULTS AND DISCUSSION

A. Orientation dynamics starting from the ground rotational state

Based on the method described in the previous section, we performed simulations using HBr as the target molecule. HBr is a polar molecule with a moderate permanent dipole moment of $\mu_0 = 0.828$ debye [27] and a polarizability anisotropy of $\Delta\alpha = 0.91$ Å^3 [28]. The rotational constant in its vibronic ground state and the rotational period are $B_e = 8.3482$ cm^{-1} [27] and $\tau_{\rm rot} = 2.0$ ps, respectively. We set the peak electric-field amplitude of the femtosecond laser pulse as 0.116 GV/cm, which corresponds to the intensity of 18 TW/cm^2, and the pulse duration as 100 fs FWHM in intensity. The temporal shape and power spectrum of the THz pulse is shown in Fig. 1(b). The peak electric-field amplitude, the pulse duration, and the central frequency of the THz pulse are 0.76 MV/cm, 500 fs FWHM in intensity, and 1.0 THz, respectively. These values are taken from a recent experiment on the generation of an intense THz pulse reported by Watanabe *et al.* [25].

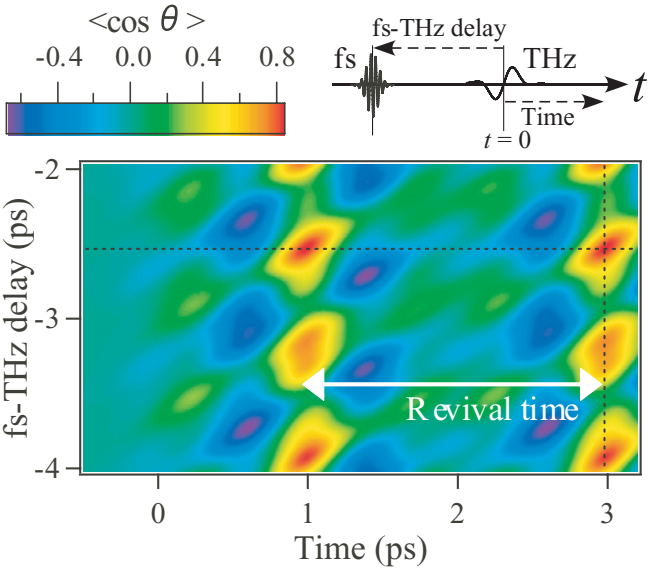

FIG. 2. (Color online) Two-dimensional plot of orientation dynamics with respect to the time delay between the femtosecond and THz pulses (y axis), and the time after the irradiation of the THz pulse (x axis). The timings for the maximal orientation are indicated by dashed lines.

Figure 2 shows the calculated results of the orientation parameter $\langle\cos\theta\rangle$ obtained by assuming that the HBr molecule is initially in its ground rotational state, $|J,M\rangle = |0,0\rangle$. The horizontal axis in Fig. 2 represents a time where we define the envelope peak of the THz pulse as an origin of the coordinate. The vertical axis represents a time delay of the femtosecond laser pulse with respect to the THz pulse. The time ranges of both axes in Fig. 2 are set longer than the full revival time to show all of the information for understanding the orientation dynamics. The maximal orientation value under field-free conditions reaches $\langle\cos\theta\rangle_{\max} = 0.84$ at the time delay of -2.53 ps and the time of 2.98 ps. In our simulations, $\langle\cos\theta\rangle > 0$ corresponds to the case when H atoms are directed in the positive direction of the laboratory-fixed Z axis, i.e., the positive direction of THz fields in Fig. 1(b). The minimal value, which corresponds to the orientation directed in the negative direction, is estimated to be $\langle\cos\theta\rangle_{\min} = -0.66$. Thus the orientation dynamics is asymmetric, although the maximal field amplitudes are equal in positive and negative directions, as shown in Fig. 1(b). This is because the THz pulse is not symmetric about the time reversal in the sense that the field becomes first negative then positive. The only way to achieve $\langle\cos\theta\rangle_{\min} = -0.84$ is to reverse the sign of the THz field, which means that the field becomes first positive then negative. The obtained value of $|\langle\cos\theta\rangle| = 0.84$ is close to the optimized value of $|\langle\cos\theta\rangle|\approx 0.9$ when a HCP is combined with a femtosecond laser pulse [21,22]. We performed another simulation with the same parameters but without the femtosecond laser pulse. In this case, the maximum orientation parameter was $|\langle\cos\theta\rangle|_{\max} = 0.38$. Thus we conclude that the preexcitation with the femtosecond laser pulse enhances the degree of molecular orientation.

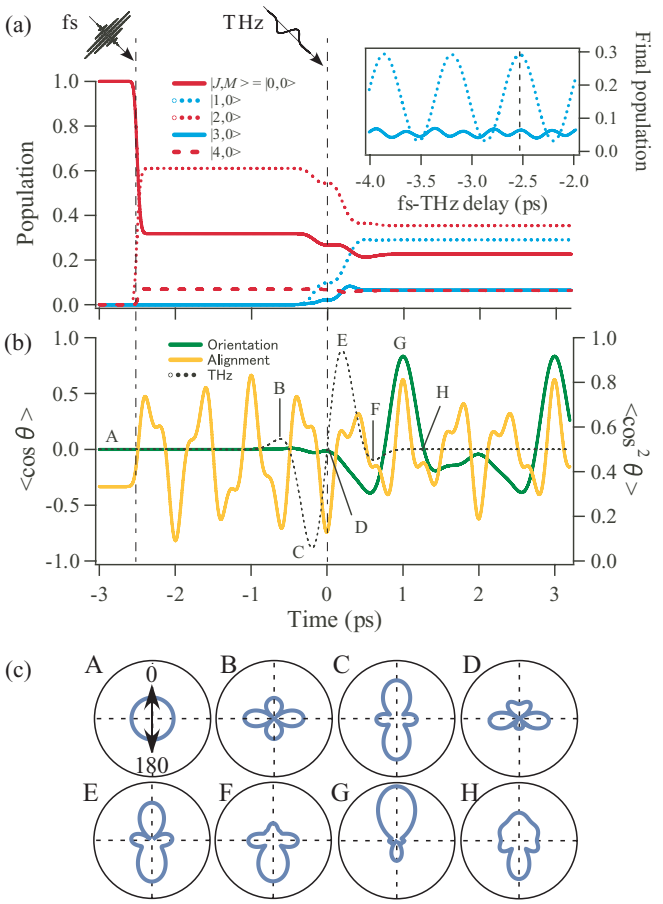

FIG. 3. (Color online) (a) Time evolution of the populations of rotational states when femtosecond and THz pulses are irradiated at −2.53 and 0 ps, respectively. Inset: Plot of populations of $J = 1$ and 3 after the irradiation of femtosecond and THz pulses as a function of the time delay. The time delay of −2.53 ps is indicated by a dashed line. (b) Time evolution of degrees of orientation ($\langle\cos\theta\rangle$) and alignment ($\langle\cos^2\theta\rangle$). The electric field of the THz pulse is indicated by a dashed line. (c) Angular distributions at different times indicated in (b). The polarization axis of femtosecond and THz pulses is indicated by a double-headed arrow in A. Note that $|\psi(\theta,t)|^{\frac{2}{3}}$ is plotted as a radial component to show the angular structure clearly.

We now analyze the orientation mechanism by tracking both populations and phases of the rotational states. Figure 3(a) shows the time evolution of the populations of rotational states at the time delay of −2.53 ps. First, the molecules are excited to $J = 2,4$ states by the femtosecond pulse and then transferred to $J = 1,3$ by the THz pulse, as shown in Fig. 3(a). After the irradiation of both pulses, the populations remain unchanged, whereas the orientation degree, which depends on both populations and relative phases, starts increasing, as plotted in Fig. 3(b). Maximal orientation is achieved when the relative phases of the related states from $J = 0$ to 4 become nearly identical. These phases lie within 16 degrees at the time of 2.98 ps. In the inset of Fig. 3(a), the final populations of the $J = 1,3$ states after THz radiation are given as a function of the time delay, where the periodic modulations arise from the coherent evolution of several even J states that are excited by the femtosecond laser pulse. At the time delay of −2.53 ps, the populations of $J = 1,3$ states peak simultaneously. At this time delay, the degree of orientation is calculated to be maximum by the previous simulation in Fig. 2. Therefore, the population transfer to odd J states is a crucial point to achieve a higher degree of orientation. This result agrees well with the discussion in Sec. II C.

Similar simulations have been performed using HCPs in several studies [19–23]. In these HCPs methods, (i) the pulse width is assumed to be much shorter than the rotational periods of molecules, and (ii) the rotational motion during the pulse is neglected: this is called the sudden-impact approximation. Then, an asymmetric polarity, which is given by an integration of the electric field, imparts an asymmetric torque to orient molecules. While this model succeeded in simulating the orientation dynamics triggered by HCPs, it is not suitable in our case. This is because, under this approximation, an alternating THz field cannot give any asymmetric torque. In our method, the molecules are resonantly excited by the THz pulse because the energy spacings between neighboring rotational states are comparable to the frequency components of the THz pulse, as shown in Fig. 1. This means that acceleration or deceleration of molecular rotational motion occurs during the THz pulse, and the molecules are not stationary anymore. Moreover, the angular distribution of the molecules changes rapidly in the presence of the THz field because the rotational wave packets are created by preexcitations. Therefore, the optimization of the intensity and timing of both femtosecond laser and THz pulses is crucial to realize the appropriate superposition for higher orientation.

Figure 3(b) shows the evolution of the degrees of molecular orientation $\langle\cos\theta\rangle$ and alignment $\langle\cos^2\theta\rangle$. At the center of the THz pulse (marked as D), the molecules are anti-aligned [22]. This result can be derived analytically by applying first-order perturbation theory (see Appendix). After irradiation by the THz pulse, the orientation and alignment are enhanced simultaneously (marked as G). This suggests that the asymmetric torques are efficiently imparted to molecules by the THz field. The angular distributions of the rotational wave packets at the times denoted by A–H in Fig. 3(b) are depicted in Fig. 3(c). In the presence of the THz field, the angular distributions of the rotational wave packets drastically change and subtle anisotropic distributions are already observed during the THz pulse (D–F). At time G, a large anisotropic angular distribution is obtained. As the time moves from G to H, the anisotropic distribution persists even when the orientation parameter $\langle\cos\theta\rangle$ reduces to zero.

Finally, it should be noted that the achieved orientation in Fig. 3(b) has a finite duration of 280 fs for $\langle\cos\theta\rangle > 0.5$. A detailed discussion about the relation between the maximum degree of post-pulse orientation and its duration is given in Ref. [23]. From the viewpoint of applications, the achieved duration is long enough to probe electron dynamics via photoemission or high harmonic generation, or vibrational dynamics using femtosecond laser pulses.

B. Optimal intensity and the carrier-envelope phase (CEP) of the THz pulse

First, we examine the effect of THz pulse intensity on the orientation mechanism. We changed the peak electric-field

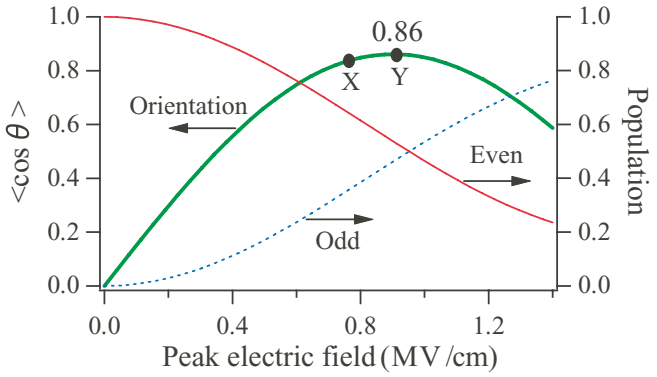

FIG. 4. (Color online) Degree of orientation (green, thick curve) and total populations of even J (red, thin curve) and odd J (blue, dashed curve) states after the THz pulse excitation as a function of the peak amplitude of the THz electric field. The strength used in the calculations in Fig. 2 is indicated by X, and the one with which the orientation degree is saturated at ∼0.86 is indicated by Y.

amplitudes of the THz pulse, while maintaining the same temporal wave form as the one shown in Fig. 1(b) and the same parameters for the femtosecond pulse. We calculated the values of $\langle\cos\theta\rangle$ at the time delay of −2.53 ps and the time of 2.98 ps, which gave the maximum orientation in the previous section. The calculated results are given in Fig. 4. In the weak-THz-field regime below 0.5 MV/cm, $\langle\cos\theta\rangle$ increases almost linearly with the field amplitude. This is because the Hamiltonian in Eq. (2) includes a linear term of the electric field. The intensity of the THz pulse used in the calculations in Fig. 2 is indicated by X in Fig. 4. To understand the saturation effect that occurred around Y in Fig. 4, we calculated the total populations of the even and odd J states after the excitation by the THz pulse. The even and odd populations are defined as $P_{\rm even} = \sum_{J:\rm even} |\langle J,0|\psi(t)\rangle|^2$ and $P_{\rm odd} = \sum_{J:\rm odd} |\langle J,0|\psi(t)\rangle|^2$. These values after the excitation by the THz pulse are plotted in Fig. 4. The saturation effect of the orientation occurs near the crossing point of the even and odd populations where the prefactors of cosine in Eq. (5) become maximum. This result is consistent with the case of simple two-level and three-level rotational systems. When only the two lowest-lying rotational states $|J,M\rangle = |0,0\rangle$ and $|1,0\rangle$ are involved, a maximal orientation value of $|\langle\cos\theta\rangle|_{\rm max} = 0.58$ is achieved by the superposition of $|\psi\rangle = 1/\sqrt{2}|0,0\rangle + 1/\sqrt{2}|1,0\rangle$. Similarly, when the three rotational states $|J,M\rangle = |0,0\rangle, |1,0\rangle$, and $|2,0\rangle$ are involved, $|\langle\cos\theta\rangle|_{\rm max} = 0.77$ is achieved by the superposition of $|\psi\rangle = \sqrt{10}/6|0,0\rangle + 1/\sqrt{2}|1,0\rangle + \sqrt{2}/3|2,0\rangle$. In both two- and three-level systems, maximal orientations are achieved when $P_{\rm even} = P_{\rm odd} = 0.5$. As can be seen above, the optimum intensity of the THz pulse to maximize orientations is obtained when $P_{\rm even}$ and $P_{\rm odd}$ come close to each other.

Next, we examined how the CEP of the THz pulse affects orientation dynamics. We changed the CEP of the THz pulse from 0 to 2π with a step of $\pi/10$ and conducted the simulation with the same parameters. To shift the CEP while maintaining the same THz spectrum as shown in Fig. 1(b), we multiplied a phase offset with the THz spectrum in a frequency domain and then Fourier transformed it back to obtain the temporal wave form. The time integration of each pulse was checked to be zero by numerically integrating it in the time window of our interest. Despite the drastic changes in the THz pulse shape, magnitudes of the maximal orientation value, $|\langle\cos\theta\rangle|_{\rm max}$, marginally changed between 0.80 and 0.84. This can be attributed to the fact that the molecular orientation is achieved by the resonant transition induced by the THz pulse, and not by the asymmetric polarity as in the case of HCPs [19–23]. Therefore, the orientation degree is mainly determined by the spectral intensities and relative phases of resonant frequency components, and is less influenced by the CEP.

C. Orientation dynamics at finite temperatures

In the previous section, we investigated the orientation dynamics of HBr, which was initially in its ground rotational state, by assuming a zero rotational temperature. However, in the real experiments, the molecular ensemble is at finite temperatures and multiple rotational states are populated incoherently. The thermally averaged orientation dynamics is given as follows [26]:

$$\langle\langle\cos\theta\rangle\rangle(t) = Q^{-1}\sum_{J=0}^{J_{\rm max}}\exp\left[-\frac{B_{\rm e}J(J+1)}{k_{\rm B}T}\right] \times \sum_{M=-J}^{J}\langle\cos\theta\rangle_{J,M}(t), \quad (7)$$

where

$$Q = \sum_{J=0}^{J_{\rm max}}(2J+1)\exp\left[-\frac{B_{\rm e}J(J+1)}{k_{\rm B}T}\right] \quad (8)$$

is the partition function. $k_{\rm B}$ and T are the Boltzmann constant and the initial rotational temperature, respectively. $\langle\cos\theta\rangle_{J,M}(t)$ expresses the orientation dynamics starting from the $|J,M\rangle$ initial state. We used the same parameters for both pulses and time delay as used in the results shown in Fig. 2, and the calculated dynamics is given in Fig. 5 for the temperatures $T = 1$, 10, and 20 K. The inset of the figure shows the initial distributions of the rotational states at these temperatures. At $T = 1$ K, almost all molecules are distributed on $J = 0$,

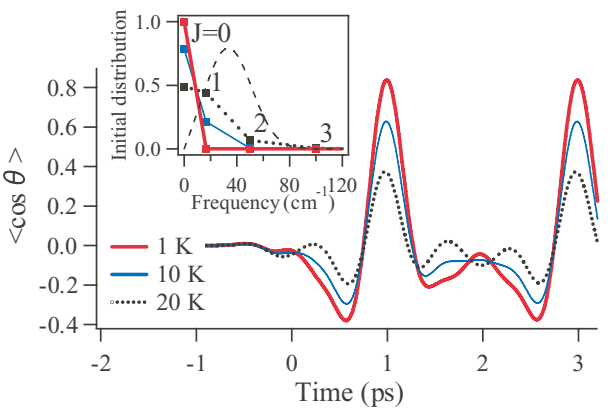

FIG. 5. (Color online) Effects of initial temperature on the degree of orientation. Inset: Distribution of rotational states at 1 K (red, thick curve), 10 K (blue, thin curve), and 20 K (black, dotted curve), respectively; the THz pulse spectrum is shown by the dashed line.

whereas at $T = 20$ K, the initial distributions of $J = 1,2$, and 3 (different M states are summed for each J state) are 0.489, 0.442, and 0.067, respectively. At all initial temperatures, less than 1% of the entire population is distributed on $J > 3$ states. Although the efficiency of orientations decreases with increasing initial temperatures, $\langle \cos\theta \rangle_{\max} > 0.6$ is achieved at $T = 10$ K. Such rotationally cold molecules can be prepared with a supersonic expansion technique. The time that gives the maximum orientations does not depend on the initial rotational temperatures and is nearly fixed at half of the rotational period. This robustness against rotational temperature clearly suggests the feasibility of the proposed method with HBr molecules.

IV. CONCLUSION

We proposed a method to realize a high degree of molecular orientation using a single-cycle intense THz pulse combined with preexcitation by a nonresonant, intense femotosecond laser pulse. The optimum intensity of the THz pulse is calculated to be on the order of 1 MV/cm, which is experimentally accessible with current laser technologies [25]. The dependencies on other experimental parameters such as the CEP and finite temperature effects are numerically examined, showing the robustness of the method. Essentially, it is important to preexcite molecules to high rotational states by a femtosecond laser pulse so that the energy spacing between neighboring rotational states, $\Delta E_{J+1,J} = B_e(J+1)$, becomes comparable to the frequency component of the THz pulse. Because of this straightforward strategy, our method is not limited to small molecules such as HBr and is applicable to larger molecules. For this purpose, the optical centrifuge technique [29], in which molecules are trapped within a narrow range of high J states, might be useful. Moreover, the spectral range of the THz pulse might be extended from a few to several tens of THz. Such pulses can be achieved using differential frequency generation [30]. The high-field amplitude associated with the good focusability of the high-frequency THz field will enable a higher degree of orientation in a wide range of polar molecules.

ACKNOWLEDGEMENT

This research was partially supported by the Photon Frontier Network Program of the Ministry of Education, Culture, Sports, Science and Technology, Japan.

APPENDIX

The inset of Fig. 3(a) suggests that the optimum time delay of fs and THz pulses corresponds to the time when the final populations of $J = 1,3$ states become maximum. We will derive analytically that this condition is satisfied when the wave packets are anti-aligned at the center of the sine-shaped THz pulse (i.e., the envelope peak of the THz pulse coincides with the timing of anti-alignment) as shown in Figs. 3(b) and 3(c). For simplicity, we assume molecules are initially in the ground rotational state and focus on the $J = 1$ state. A similar discussion is applicable to the $J = 3$ state. First, we express the wave packets after the fs pulse as

$$|\psi(t)\rangle = \sum_{J=0}^{J_{\max}} c_J^{\mathrm{fs}} |J\rangle \exp\left(-i\frac{E_J}{\hbar}t\right), \tag{A1}$$

where c_J^{fs} is a coefficient of the rotational eigenstate after the fs pulse excitations. They are complex numbers and the relative phases of eigenstates are included there. Next, we apply first-order perturbation theory and assume that only single, not sequential, dipole transition occurs during the interaction with the THz pulse, as shown in Fig. 1(a). Then the coefficient of the $J = 1$ state after the THz pulse, c_1^{THz}, can be calculated by a coherent sum of the two excitation pathways of $J = 0 \to 1$ and $J = 2 \to 1$ as

$$\begin{aligned} c_1^{\mathrm{THz}} \propto\ & \langle 1|\cos\theta|0\rangle \varepsilon_{\mathrm{THz}}(\omega_{1,0}) c_0^{\mathrm{fs}} \\ & + \langle 1|\cos\theta|2\rangle \varepsilon_{\mathrm{THz}}(\omega_{2,1})^* c_2^{\mathrm{fs}}, \end{aligned} \tag{A2}$$

where $\omega_{J',J} = \Delta E_{J',J}/\hbar$, and $\varepsilon_{\mathrm{THz}}(\omega)$ is related with $\varepsilon_{\mathrm{THz}}(t)$ by the following equation:

$$\varepsilon_{\mathrm{THz}}(t) = 2\,\mathrm{Re}\int_0^\infty \varepsilon_{\mathrm{THz}}(\omega)\exp(-i\omega t)\,d\omega. \tag{A3}$$

For a sine-shaped THz pulse, $\arg[\varepsilon_{\mathrm{THz}}(\omega_{1,0})] = \pi/2$ and $\arg[\varepsilon_{\mathrm{THz}}(\omega_{2,1})^*] = -\pi/2$. When the relative phase between c_0^{fs} and c_2^{fs} equals π on the complex plane, the two terms in Eq. (A2) interfere positively. By substituting this condition into Eq. (A1), the relative phase of the $J = 0,2$ states at $t = 0$ is derived to be π. Similarly, the population of the $J = 3$ state becomes maximum when the relative phase of the $J = 2,4$ states at $t = 0$ is equal to π. These results suggest that when the sine-shaped THz pulse is irradiated at the timing of anti-alignment of the rotational wave packets, the populations of odd J states are enhanced coherently. Thus we can induce the maximum degree of orientation after a certain time in a field-free condition. This analysis is consistent with the numerical results in Figs. 3(b) and 3(c).

[1] H. Stapelfeldt and T. Seideman, Rev. Mod. Phys. **75**, 543 (2003).
[2] H. Sakai, C. P. Safvan, J. J. Larsen, K. M. Hilligsøe, K. Hald, and H. Stapelfeldt, J. Chem. Phys. **110**, 10235 (1999).
[3] F. Rosca-Pruna and M. J. J. Vrakking, Phys. Rev. Lett. **87**, 153902 (2001).
[4] Y. Ohshima and H. Hasegawa, Int. Rev. Phys. Chem. **29**, 619 (2010).
[5] D. Pavičić, K. F. Lee, D. M. Rayner, P. B. Corkum, and D. M. Villeneuve, Phys. Rev. Lett. **98**, 243001 (2007).
[6] R. Velotta, N. Hay, M. B. Mason, M. Castillejo, and J. P. Marangos, Phys. Rev. Lett. **87**, 183901 (2001).
[7] J. Itatani, D. Zeidler, J. Levesque, M. Spanner, D. M. Villeneuve, and P. B. Corkum, Phys. Rev. Lett. **94**, 123902 (2005).

[8] K. Kitano, H. Hasegawa, and Y. Ohshima, Phys. Rev. Lett. **103**, 223002 (2009); Y. Khodorkovsky, K. Kitano, H. Hasegawa, Y. Ohshima, and I. S. Averbukh, Phys. Rev. A **83**, 023423 (2011).
[9] J. Itatani, J. Levesque, D. Zeidler, H. Niikura, H. Pépin, J. C. Kieffer, P. B. Corkum, and D. M. Villeneuve, Nature (London) **432**, 867 (2004).
[10] M. Meckel *et al*., Science **320**, 1478 (2008).
[11] H. J. Loesch and A. Remscheid, J. Chem. Phys. **93**, 4779 (1990).
[12] D. H. Parker and P. B. Bernstein, Annu. Rev. Phys. Chem. **40**, 561 (1989).
[13] B. Friedrich and D. Herschbach, J. Chem. Phys. **111**, 6157 (1999).
[14] H. Sakai, S. Minemoto, H. Nanjo, H. Tanji, and T. Suzuki, Phys. Rev. Lett. **90**, 083001 (2003)
[15] L. Holmegaard, J. H. Nielsen, I. Nevo, H. Stapelfeldt, F. Filsinger, J. Küpper, and G. Meijer, Phys. Rev. Lett. **102**, 023001 (2009).
[16] S. De *et al*., Phys. Rev. Lett. **103**, 153002 (2009).
[17] K. Oda, M. Hita, S. Minemoto, and H. Sakai, Phys. Rev. Lett. **104**, 213901 (2010).
[18] O. Ghafur, A. Rouzée, A. Gijsbertsen, W. K. Siu, S. Stolte, and M. J. J. Vrakking, Nature Phys. **5**, 289 (2009).
[19] M. Machholm and N. E. Henriksen, Phys. Rev. Lett. **87**, 193001 (2001).
[20] C. M. Dion, A. Keller, and O. Atabek, Eur. Phys. J. D **14**, 249 (2001); A. Matos-Abiague and J. Berakdar, Phys. Rev. A **68**, 063411 (2003); C. C. Shu, K. J. Yuan, W. H. Hu, and S. L. Cong, *ibid*. **80**, 011401(R) (2009); J. Chem. Phys. **132**, 244311 (2010).
[21] D. Daems, S. Guérin, D. Sugny, and H. R. Jauslin, Phys. Rev. Lett. **94**, 153003 (2005).
[22] E. Gershnabel, I. S. Averbukh, and R. J. Gordon, Phys. Rev. A **74**, 053414 (2006).
[23] D. Sugny, A. Keller, O. Atabek, D. Daems, C. M. Dion, S. Guérin, and H. R. Jauslin, Phys. Rev. A **69**, 033402 (2004).
[24] J. Hebling, G. Almási, I. Z. Kozma, and J. Kuhl, Opt. Express **10**, 1161 (2002); K.-L. Yeh, M. C. Hoffmann, J. Hebling, and K. A. Nelson, Appl. Phys. Lett. **90**, 171121 (2007).
[25] S. Watanabe, N. Minami, and R. Shimano, Opt. Express **19**, 1528 (2011).
[26] J. Salomon, C. M. Dion, and G. Turinici, J. Chem. Phys. **123**, 144310 (2005).
[27] NIST Database; [http://webbook.nist.gov/chemistry/].
[28] J. O. Hirschfelder, C. F. Curtiss, and R. B. Bird, *Molecular Theory of Gases and Liquids* (Wiley, New York, 1954).
[29] J. Karczmarek, J. Wright, P. Corkum, and M. Ivanov, Phys. Rev. Lett. **82**, 3420 (1999); D. M. Villeneuve, S. A. Aseyev, P. Dietrich, M. Spanner, M. Y. Ivanov, and P. B. Corkum, *ibid.* **85**, 542 (2000); M. Spanner and M. Y. Ivanov, J. Chem. Phys. **114**, 3456 (2001).
[30] S. Alexander, A. Leitenstorfer, and R. Huber, Opt. Lett. **33**, 2767 (2008).